Journal of Nanobiotechnology

RESEARCH

Open Access

The immunogenic potential of an optimized mRNA lipid nanoparticle formulation carrying sequences from virus and protozoan antigens

Renata S. Fernandes[1], Gabriela de Assis Burle-Caldas[1†], Sarah Aparecida Rodrigues Sergio[1], Ana Flávia Bráz[1], Nathália Pereira da Silva Leite[1], Milton Pereira[1], Juliana de Oliveira Silva[1,2], Natália Satchiko Hojo-Souza[1,3], Bianca de Oliveira[1], Ana Paula S. Moura Fernandes[1,6], Flávio Guimarães da Fonseca[1,4], Ricardo Tostes Gazzinelli[1,3,5], Diego dos Santos Ferreira[1,2] and Santuza M. Ribeiro Teixeira[1,5*]

Abstract

Background Lipid nanoparticles (LNP) are a safe and effective messenger RNA (mRNA) delivery system for vaccine applications, as shown by the COVID-19 mRNA vaccines. One of the main challenges faced during the development of these vaccines is the production of new and versatile LNP formulations capable of efficient encapsulation and delivery to cells in vivo. This study aimed to develop a new mRNA vaccine formulation that could potentially be used against existing diseases as well as those caused by pathogens that emerge every year.

Results Using firefly luciferase (Luc) as a reporter mRNA, we evaluated the physical–chemical properties, stability, and biodistribution of an LNP-mRNA formulation produced using a novel lipid composition and a microfluidic organic-aqueous precipitation method. Using mRNAs encoding a dengue virus or a *Leishmania infantum* antigen, we evaluated the immunogenicity of LNP-mRNA formulations and compared them with the immunization with the corresponding recombinant protein or plasmid-encoded antigens. For all tested LNP-mRNAs, mRNA encapsulation efficiency was higher than 85%, their diameter was around 100 nm, and their polydispersity index was less than 0.3. Following an intramuscular injection of 10 µg of the LNP-Luc formulation in mice, we detected luciferase activity in the injection site, as well as in the liver and spleen, as early as 6 h post-administration. LNPs containing mRNA encoding virus and parasite antigens were highly immunogenic, as shown by levels of antigen-specific IgG antibody as well as IFN-γ production by splenocytes of immunized animals that were similar to the levels that resulted from immunization with the corresponding recombinant protein or plasmid DNA.

Conclusions Altogether, these results indicate that these novel LNP-mRNA formulations are highly immunogenic and may be used as novel vaccine candidates for different infectious diseases.

Keywords mRNA vaccine, Lipid nanoparticles, Dengue, Leishmaniasis, Biodistribution, IgG, IFNγ

†Renata S. Fernandes and Gabriela de Assis Burle-Caldas have contributed equally to this work.

*Correspondence:
Santuza M. Ribeiro Teixeira
santuzat@ufmg.br
Full list of author information is available at the end of the article

Graphical Abstract

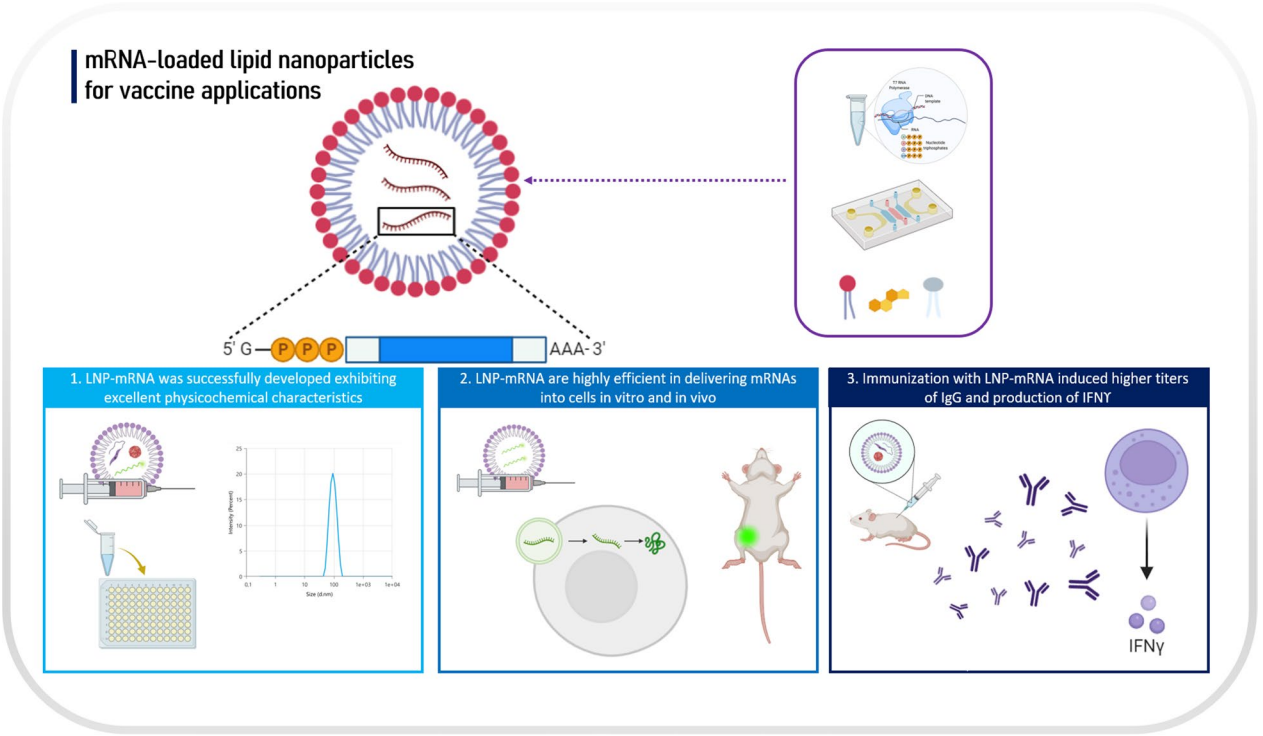

Background

Following the discovery of interference RNA, the RNA molecule has garnered significant attention as a molecule that can be explored for its therapeutic applicability [1]. Propelled by the recent success of SARS-CoV-2 mRNA lipid nanoparticle vaccines (Moderna and Pfizer–BioNTech), messenger RNA (mRNA) has taken an even more prominent place in therapeutics [2]

mRNA vaccines offer several advantages over other types of vaccines. Their development is notably swift, facilitated by LNP-mRNA functioning as a versatile platform technology. These vaccines can be produced rapidly, with reduced costs, employing a common manufacturing platform and purification methods irrespective of the antigen. Furthermore, mRNA platforms are safer and easier to deliver compared to DNA vaccines, as they do not require crossing the nuclear membrane and do not integrate or alter the genome [3–6].

Nevertheless, a significant hurdle in mRNA vaccine development is the inherent instability and immunogenicity of the RNA molecule. The immunostimulatory issues of in vitro transcribed RNA were resolved by Kariko et al.'s groundbreaking study, which developed an mRNA synthesis protocol with modified nucleosides. [7]. The mRNA structure is optimized by adding a 5' cap and identifying suitable 5' and 3' untranslated sequences to further enhance stability and translation efficiency. [8, 9]. To enhance the mRNA in vivo stability after its administration, great efforts have been made to create a delivery system that not only protects the molecule against degradation but also allows it to overcome tissue and cell barriers to be delivered into the cytoplasm. Consequently, successful mRNA vaccines result from studies that led to both proficient delivery of mRNA and subsequent antigen expression to promote antigen-specific immunity [10, 11]. Lipid nanoparticles (LNP) are at the forefront of technologies designed to encapsulate and protect mRNA [12, 13]. LNP encapsulation mitigates premature mRNA degradation and improves its delivery to the cytosol of antigen-presenting cells (APC) [14, 15].

LNP, the most effective adopted delivery approach, is typically composed of an ionizable lipid, a phospholipid, a sterol, and a lipid-anchored polyethylene glycol (PEG) [13, 16]. Each lipid has a specific function, including mRNA encapsulation, disruption of the endosomal membrane, cellular delivery, formation and stabilization of the lipid bilayer, homogeneity of particle

size and dispersity, particle stability during preparation and storage, circulation half-life, and biodistribution [16–20].

Although LNP preparation can be performed in various ways, microfluidic methods are preferred for preclinical and clinical studies due to their superior reproducibility. LNP are formed when solubilized lipids in the organic phase are submitted to a rapid increase in the dispersion media's polarity induced by swiftly mixing it with an aqueous phase containing mRNA. This rapid mixing leads to the supersaturation of lipid molecules, resulting in the self-assembly of LNPs. mRNA encapsulation occurs through the electrostatic association between negatively charged nucleic acids and positively charged lipids. As mRNAs encoding different antigens are chemically and physically highly similar, new mRNA vaccines' formulation design and manufacturing processes follow the same steps [21–23].

mRNA vaccines stimulate the innate immune system and deliver mRNA to APC for antigen expression [24]. APC uptake mRNA-loaded LNP, express the protein, and migrate to lymph nodes to prime T cells [25, 26]. LNP intrinsically activates APC-like dendritic cells, macrophages, and B cells, acting as potent adjuvants [27–31]. Recent studies showed that both empty LNP and mRNA-loaded LNP elicit the production of several chemokines and cytokines in higher levels than AddaVax-adjuvanted protein vaccines and is likely the mechanistic basis for the LNP potent adjuvant activity [24, 32].

In vivo antigen production achieved with mRNA vaccines, coupled with the self-adjuvant properties of LNP-mRNA vaccines, ultimately leads to the efficient generation of strong humoral and cellular immunity [10, 33]. In the present study, we developed a new mRNA vaccine formulation that could potentially be used against existing diseases as well as those caused by novel pathogens that emerge every year. After evaluating the physicochemical characteristics and biodistribution using an LNP containing luciferase mRNA, we assessed the immunogenic potential of two LNP-mRNA formulations containing mRNAs encoding 80% of the dengue serotype 3 E protein (E80) as well as an antigen derived from *Leishmania infantum* (LinKAP), and compared the immune response with the corresponding plasmid DNA and recombinant protein, respectively. The results indicate that immunization with the LNP-mRNA formulations resulted in humoral and cellular immune responses that are similar to the responses elicited by the corresponding plasmid DNA and recombinant protein and may be used as novel vaccine candidates for different infectious diseases.

Material and methods

Material

MEGAscriptT7 Transcription Kit was obtained from Thermo Fischer. CleanCap and N^1-Methylpseudouridine-5'-Triphosphate were purchased from TriLink. DODMA (1,2-dioleyloxy-3-dimethylaminopropane), DSPC (1,2–distearoyl-sn-glycero-3-phosphocholine), and DMG-PEG-2000 (1,2-dimyristoyl-rac-glycero-3-methoxypolyethylene glycol-2000) were obtained from Avanti Polar Lipids. Cholesterol and sulforhodamine B (SRB) were purchased from Sigma-Aldrich. Quant-iT™ RiboGreen™ RNA Reagent and Kit were obtained from Invitrogen. D-luciferin, reporter lysis 5X buffer, and VivoGlo were provided by Promega. Dulbecco's Modified Eagle's Medium (DMEM), fetal bovine serum, trypsin EDTA, and PBS 1X buffer were purchased from Gibco-Invitrogen. All other chemicals were of analytical and/or molecular biology grade.

Synthesis of nucleoside-modified mRNAs

Codon-optimized sequences corresponding to part of the *L. infantum* antigen LinKAP (LINF_270007500, www.trytripDB.org) and 80% of the consensus E serotype 3, genotype BR-III sequence (E80) from circulating strains of dengue virus in Brazil during 2007–2021, were synthesized by GeneScript in the pcDNA3.1 plasmid containing appropriated 5' and 3' UTRs and a 110 nt poly-A tail (Figure S1). We used the truncated 80% E protein of the Dengue virus, instead of the full-length sequence, because the removal of a transmembrane, hydrophobic region does not compromise the immunogenicity but significantly enhances recombinant protein expression and secretion. The MEGAscriptT7 Transcription Kit (Thermo Fischer, AM1334) was used for mRNA synthesis, and 5' cap 1 was inserted with CleanCap AG (TriLink, N-7113). Uridine was replaced by N^1-methylpseudouridine-5'-Triphosphate (TriLink, N-1081), and the reaction was performed at 37 °C for 4 h.

LNP preparation

LNP formulations were produced using the nanoprecipitation method. The organic phase was composed of a cationic ionizable lipid (1,2-dioleyloxy-3-dimethylaminopropane—DODMA), 1,2—distearoyl-sn-glycero-3-phosphochoLine (DSPC), 1,2-dimyristoyl-rac-glycero-3-methoxypolyethylene glycol-2000 (DMG-PEG2000), obtained from Avanti Polar Lipids and cholesterol (Sigma) dissolved in ethanol (in a molar ratio of 50:10:1.5:38,5, total molar concentration, N/P ratio 6:1). The aqueous phase was formed by mRNA in 20 mM citrate buffer, pH 4.0. Organic and aqueous

phases were combined in a microfluidic device (ANP, Particle Works, UK) at a flow ratio of 1:3 (ethanol: aqueous phase) in a total flow ratio of 12 mL/min. The corresponding mRNAs for dengue serotype 3 E80 protein (LNP-E80), *L. infantum* LinKAP antigen (LNP-LinKAP), and firefly luciferase (LNP-Luc) were used for encapsulation. All LNP were ultrafiltered using Amicon centrifugal devices (30 KDa) and resuspended in PBS buffer, pH 7.4, before use.

LNP and LNP-mRNA characterization

The particle size, polydispersity index (PDI), and zeta potential of LNP-mRNA were measured by dynamic light scattering (DLS) at a fixed angle of 90º and 25ºC using a Zetasizer Nano ZS90 (Malvern Instruments, UK). Nanoparticle Tracking Analysis (NTA) was conducted using NanoSight NS300 & NTA 3.1 Analytical Software (Malvern Instruments, UK). A laser source and light scattering irradiated the suspension, and a charge-coupled device camera was used to capture images. Quant-iT™ RiboGreen™ RNA Reagent and Kit (Invitrogen) was used to assess the encapsulation efficiency and mRNA concentration of LNP-mRNA. Fluorescence was measured in a formulation freshly prepared in the presence or absence of Triton X100. The integrity of mRNA after the encapsulation into LNP was confirmed by mRNA extraction with phenol–chloroform, followed by denaturing agarose gel electrophoresis. The morphology of LNP-mRNA was analyzed by cryogenic transmission electron microscopy (cryo-TEM) using the plunge freezing technique whereby the samples were spread on a thin film across an EM grid and submerged in liquid ethane.

Freeze and thaw stability of LNP-mRNA.

To determine the preliminary freeze and thaw stability of LNP-Luc, the nanoparticles were prepared as described in 2.2. After ultrafiltration, the obtained nanoparticles were resuspended in Tris–HCl buffer pH 7.4 (20 mM) containing sucrose 12% (w/v) as a cryoprotectant. Nanoparticle aliquots were then stored at 4 °C, -20 °C, and -80 °C, and samples were collected at one- and seven days post-preparation. As previously outlined, mean diameter, PDI, zeta potential, encapsulation efficiency, and mRNA integrity were evaluated. To verify if luciferase activity was also preserved after LNP-mRNA storage, 10 µg of LNP-Luc was injected in mice via the intramuscular (IM) route, and bioluminescence values were quantified as indicated under "Biodistribution studies."

mRNA transfection and protein expression analyses

HEK293T cells were seeded in 6-well plates at a density of 7×10^5 cells/well 24 h prior to transfection. For transfection studies with Luc-mRNA, cells were exposed to 3, 6, and 9 µg of LNP-Luc or naked mRNA without any transfection reagent. Twenty-four- and 48-h post-incubation cells were lysed with 1X cell lysis buffer for luciferase assay (Reporter Lysis 5X buffer, Promega) and centrifuged (3000 rpm, 10 min). The supernatant was collected and transferred to a 96-well plate with firefly D-luciferin reagent (Promega, E1500). Bioluminescence intensity was read in a luminometer Luminoskan (ThermoScientific).

For transfections with *Leishmania* or dengue mRNAs, cells were prepared as described previously and transfected with 3 µg of either encapsulated or naked mRNA (without any transfection reagent). The LinKAP sequence lacks a signal peptide, limiting protein detection to cell lysates. In contrast, the E80 sequence includes the human tissue plasminogen activator (TPA)-derived signal peptide that facilitates secretion, so that the protein can be detected in the culture supernatant. Forty-eight hours post-transfection, cells transfected with LNP-LinKAP were collected, and total protein extracts were produced by cell lysis in radioimmunoprecipitation assay (RIPA) buffer (ThermoScientific, 89,901). For cells transfected with E80 from dengue virus serotype 3, the culture supernatant was collected 48 h after transfections. Total protein extracts and culture supernatant were separated in acrylamide gel (12,5%) under denaturing conditions, and samples were transferred to nitrocellulose membranes and incubated with anti-LinKAP antibody (rabbit polyclonal antibody, Oliveira et al., submitted), or anti-dengue antibody (Abcam, Ab9202). Next, membranes were incubated with anti-IgG rabbit antibody conjugated with HRP or anti-IgG mouse antibody conjugated with HRP and revealed with ECL reagent (Cytiva, RPN2236). Images were captured with a ChemiDoc Imaging System (BIO-RAD).

Cytotoxicity studies

The potential toxicity of mRNA and LNPs was assessed using sulforhodamine B (SRB) assay. HEK 293 T cells were seeded in 96-well plates at a density of 4×10^4 cells/well 24 h prior to treatment. Cells were exposed to LNP-mRNA, naked-mRNA, or blank-LNP (125–1000 ng). DMSO was used as a positive control for cellular toxicity. Twenty-four hours after the treatment, cells were fixed with 10% trichloroacetic acid (TCA) and then stained with SRB (Sigma) for 30 min. Unbound SRB was withdrawn using 1% acetic acid, while the protein-bound SRB was dissolved in 10 mM of Tris-Base [tris(hydroxymethyl) aminomethane] solution. The optical densities (OD) were measured at 510 nm on a microplate spectrophotometer Multiskan (ThermoScientific).

Biodistribution studies

Bioluminescence imaging was performed with an IVIS Spectrum imaging system (PerkinElmer). Female BALB/c mice received 10 μg of LNP-Luc via the IM route. Six, 24, 48, and 72 h post-injection, D-luciferin (VivoGlo, Promega) was administered intraperitoneally (at 100 mg/kg) in each animal. Mice were anesthetized after receiving D-luciferin in a chamber with 3% isoflurane and placed on the imaging platform while being maintained on 1% isoflurane via a nose cone. Mice were imaged at 10-min post-administration of D-luciferin using an exposure time of 5–120 s to ensure that the signal acquired was within effective detection range (above noise levels and below charge-coupled device [CCD] saturation limit). Bioluminescence values were quantified by measuring photon flux (photons/second) in the regions where a bioluminescence signal emanated using the Living IMAGE Software provided by Caliper.

Expression and purification of antigens in *E. coli*

For expression of *Leishmania* LinKAP antigen and E protein from dengue virus serotype 2, E. *coli* BL21(DE3) was transformed with plasmids pET24a or pET21a, respectively, containing the coding sequences of the antigens of interest (GeneScript). Expression of the antigen was induced for 3 to 5 h with Isopropyl β-D-1-thiogalactopyranoside (IPTG) in a final concentration of 0,5 mM at 37 ºC. After induction, bacteria were lysed using the Avestin Emulsiflex C3 Homogenizer and purification performed by affinity chromatography with His Trap HP 5 mL purification columns in ÄKTA prime plus according to the manufacturer's instructions (GE-Healthcare).

Immunization experiments

Dengue serotype 3 E80 protein and the *L. infantum* LinKAP antigen, produced in *Escherichia coli*, were used to evaluate the immunogenicity of LNP-mRNA vaccines. Female C57BL/6 or BALB/c mice were divided into groups (n = 4 and n = 5, respectively), and vaccinations were performed via IM route by injecting into the thigh muscles of the two hind limbs, 10 μg of LNP-LinKAP or LNP-E80, in 100 μl volume. Blank LNP and naked mRNA were used as negative control groups. Animals were immunized using a prime-boost or prime-boost-boost protocol with 21 days interval. For the duration of the experiment, mice were housed in ventilated cages on a 12-h dark/light cycle. The room was kept at 20 °C, 50% relative humidity. Food and water were provided ad libitum.

Quantification of total IgG and IFN-γ

Quantification of total IgG antibodies was conducted by ELISA. Plates were sensitized with 100 ng/well of recombinant LinKAP protein or 400 ng/well of recombinant E80 dengue 3 produced in eukaryotic cells (Sinobiologicals) and incubated overnight. The next day, the content was discarded, and the plates were blocked at 37 °C for one hour. The content was discarded, and the samples were added to the plate (serum from mice immunized with LNP-LinKAP was diluted at 1:100, and for E80 mRNA or DNA, 1:50) and incubated at 37 °C for one hour. After washing the plates, a specific secondary antibody was added and incubated at 37 °C for 1 h. The plates were washed again, and TMB (3.3′5.5.5-tetramethylbenzidine) was added. The reaction was interrupted with a stop solution, and the plates were read at the absorbance of 450 nm in a microplate reader (Varioskan, ThermoScientific). For quantification of IFN-*γ,* 30 days after the last immunization, the animals were euthanized, and splenocytes were isolated as described in the next section and stimulated with 10 μg/mL of LinKAP recombinant protein or E protein from dengue virus serotype 2 produced in bacteria (GenBank GU131881.1). The samples were then incubated for 72 h at 37 °C under a 5% CO_2 atmosphere. The culture supernatant was collected to determine IFN-γ levels by ELISA (Mouse IFN-γ Duo-Set ELISA, R&D System) following the manufacturer's instructions.

Splenocyte isolation and culture

For splenocyte isolation, naïve or immunized mice were euthanized using a lethal dose of anesthetics administered intraperitoneally (50 mg/kg xylazine and 500 mg/kg ketamine). Spleens were collected and macerated using a 100 μm nylon cell strainer. Splenocytes from each spleen were resuspended in 20 mL of RPMI 1640 (GIBCO) supplemented with 10% fetal bovine serum (FBS), centrifuged (400 × g, 8 min, 4 ºC), and subjected to red blood cell lysis using 5 mL of ACK lysis buffer (NH4Cl 150 mM, KHCO3 10 mM, EDTA 0.1 mM, pH 7.4) for 5 min at room temperature. The splenocytes were then washed twice with RPMI 1640 containing 10% FBS, passed through a 100 μm nylon cell strainer, and plated in a flat-bottom 96-well plate at a density of 10^6 splenocytes per well. Splenocytes isolated from immunized mice were stimulated with either the LinKAP recombinant protein or dengue serotype 2 E80 protein, both produced in bacteria. Plates were centrifuged (400 × g, 5 min, 24 ºC) and incubated for 72 h to assess IFN-γ production. For cytokine assays using lipid nanoparticles (LNPs) as stimuli, splenocytes from naïve mice were used. These plates were incubated for 16 h at 37 ºC and 5% CO_2. After

incubation, all plates were centrifuged (400 × g, 5 min, 4 °C), and the supernatants were collected for further analysis.

Cytokine assays

The levels of interleukin (IL)-6, tumor necrosis factor (TNF), IL-10, and interferon (IFN)-γ were evaluated in plasma from BALB/c mice by using BD™ Cytometric Bead Array (CBA) Mouse Th1/Th2/Th17 kit (BD, cat. 560,485). The samples were acquired in BD™ FACSVerse and analyzed on FCAP Array™ Software.

Ethics statement

All experiments with animals were carried out according to the principles of conduct of the Brazilian Guide of Practices for the Care and Use of Animals for Scientific and Didactic Purposes of CONCEA. Animal experimentation protocols were approved by the Committee on Ethics in the Use of Animals (CEUA) of Fundação Oswaldo Cruz (CEUA protocol LW34/22, LW-34/22 (P-22/22.5) and LW-3/21 (P-56/19.5)). Female WT C57BL/6 and BALB/c mice, 5–8 weeks old, were purchased from the Center for Laboratory Animal Facilities of the Universidade Federal de Minas Gerais.

Results

Characterization of LNP-mRNA formulations

The LNP-mRNA were successfully prepared by nanoprecipitation using a microfluidic device. We prepared LNPs encapsulating three distinct mRNAs: firefly luciferase mRNA (LNP-Luc), mRNA encoding dengue serotype 3 E80 protein (LNP-E80), and mRNA encoding the *L. infantum* kinetoplast-associated protein, LinKAP antigen (LNP-LinKAP). The physical–chemical parameters are shown in Fig. 1.

DLS analysis showed that the average particle size of LNP in PBS was close to 100 nm, with a low PDI (≤0,2), indicating a high degree of homogeneity among the particles and a slightly negative zeta potential (Fig. 1A-C). It was possible to achieve a high encapsulation efficiency (> 85%) for all 3 formulations, which is crucial for reaching the in vivo dose required for immunizations. LNP-mRNA particle concentration and size distribution (i.e., the mean diameter in which 10, 50, and 90% of the particles are smaller) were assessed by NTA (figure B and 1D). Consistent with the DLS analysis, the particle sizes ranged from 84 to 207 nm, with 90% of them measuring under 200 nm for all three mRNA. The particle concentration was close to 10^8 particles/ml for all three formulations.

Cryo-TEM images (Fig. 1E) revealed that the mRNA-loaded LNP particles present round, smooth-surfaced, surfaced, and nanosized particles, compatible with DLS and NTA results. A thin layer surrounding the inner bright portion, indicating the presence of a semi-structured lipid bilayer, is also observed. The presence of an electron-dense core and 'bleb' cavities in the structure indicates the localization of mRNA in the particles.

The formulation's ability to protect the mRNA from degradation was also evaluated by extracting the luciferase mRNA from the LNP-Luc and assessing its integrity using agarose gel electrophoresis (Fig. 1F). The results indicated that the LNP effectively preserved the integrity of the mRNA, as evidenced by the presence of the 1.9 kb RNA band in denaturing agarose gel electrophoresis before and after encapsulation.

Freeze–thaw stability

The efficacy of tris–HCl buffer containing 12% (w/v) sucrose as cryoprotectants was assessed comparing the physicochemical characteristics of the formulations after storage at different temperatures with a control group comprising LNP-Luc freshly formulated in PBS. Parameters such as mean diameter, PDI, zeta potential, and %EE were evaluated on both day 1 and day 7, as shown in Fig. 1G–J. Irrespective of the resuspension medium, freshly prepared LNPs consistently exhibited desirable physicochemical properties. In contrast, PBS failed to maintain these characteristics following freeze–thaw cycles. The incorporation of a cryoprotectant in LNP-mRNA formulations effectively prevented alterations in mean diameter, PDI, zeta potential, and %EE over the storage period (− 20 °C, day 1 vs. day 7), maintaining a final diameter consistently below 150 nm, and neutral surface charge. Notably, LNP-mRNA prepared with Tris–HCl containing sucrose demonstrated

(See figure on next page.)

Fig. 1 Physical–chemical characterization of LNP-mRNA. Size distribution of LNP-mRNA was measured by **a** dynamic light scattering (DLS) and **b** Nanoparticle Tracking Analysis (NTA). **c** Mean diameter, polydispersity index (PDI), zeta potential, encapsulation efficiency (%EE) for different mRNA loaded LNP **d** NTA results: mean size, distribution (D10, D50, D90), and particle concentration of LNP-Luc, LNP-LinKAP, and LNP-E80 **e** Cryo-TEM images of LNP-mRNA by plunge freezing technique **f** Analysis of Luc-mRNA in agarose gel in denaturing conditions: 1- mRNA-Luc before encapsulation and 2- mRNA-Luc after encapsulation into LNP. **g** Mean diameter, **h** PDI, **i** zeta potential, and **j** encapsulation percentage of LNP-mRNA prepared with PBS or Tris–HCl + Sucrose 12% and stored at 4 °C, -20 °C, or − 80 °C. Data are expressed by the mean (n = 3) ± standard deviation of the mean. All data were analyzed using a one-way ANOVA analysis of variance followed by Tukey's post-test. Different letters indicate significant differences among groups ($p < 0.05$)

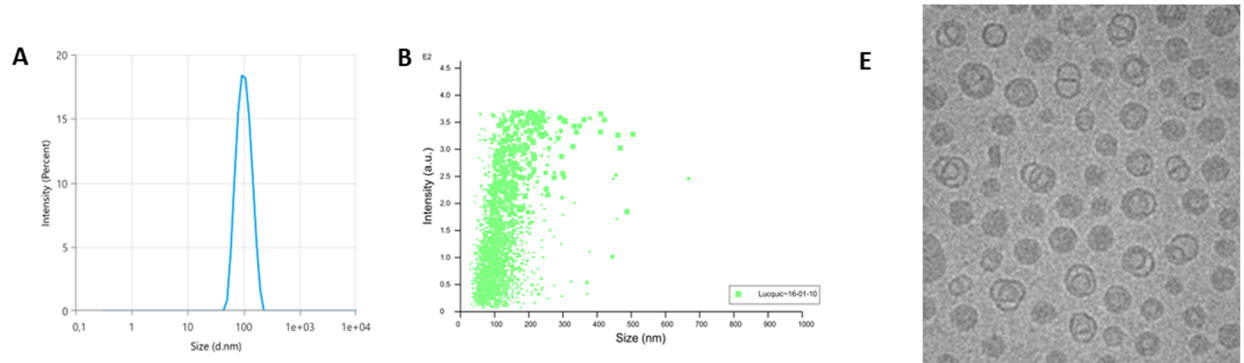

C	Mean size (nm)	PDI	Zeta potential (mV)	%EE
LNP-Luc	106.20 ± 9.26	0.17 ± 0.07	-4.80 ± 1.64	92.29 ± 1.89
LNP- LinKAP	106.05 ± 6.15	0.21 ± 0.04	-4.37 ± 2.31	86.83 ± 3.90
LNP-E80	102.16 ± 6.89	0.14 ± 0.05	-3.08 ± 2.61	92.57 ± 3.16

D	Particles/ml	Distribution (nm)		
		D10	D50	D90
LNP-Luc	$4.48x10^8$	84.6 ± 1.2	113.3 ± 3.7	199.4 ± 15.0
LNP- LinKAP	$1.07x10^9$	95.2 ± 0.9	124.8 ± 1.9	207.1 ± 4.4
LNP-E80	$1.16x10^9$	91.2 ± 1.4	121.9 ± 1.2	182.4 ± 5.2

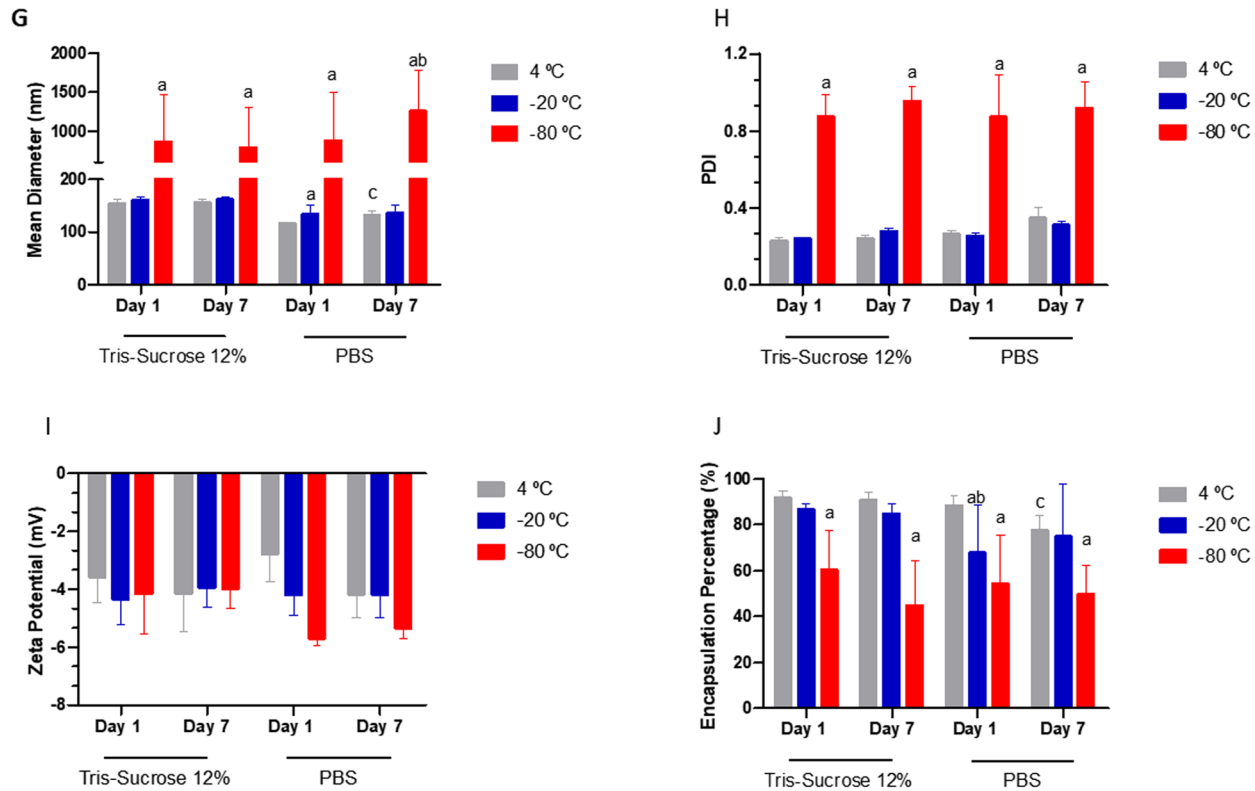

Fig. 1 (See legend on previous page.)

exceptional stability even after 7 days of storage at 4 °C, maintaining consistent mean diameter, PDI, zeta potential, %EE, and mRNA concentration, unlike LNP-mRNA prepared in PBS in which an increase in mean diameter and reduction in encapsulation efficiency were observed in the same period. Furthermore, after assessing mRNA

integrity on agarose gel electrophoresis of RNA extracted from freshly prepared LNP-mRNA and LNP-mRNA that was kept frozen at -20 °C for 7 days, we observed that freezing/thawing did not affect Luc mRNA integrity (Figure S3D).

In vitro expression and in vivo biodistribution of LNP-Luc

To verify the efficacy of mRNA delivery in vitro, we incubated HEK293T cells with 3, 6, or 9 µg of LNP-Luc for 24 h and 48 h and performed luciferase assays with the cell extracts. Cells were also incubated with 3 µg of naked

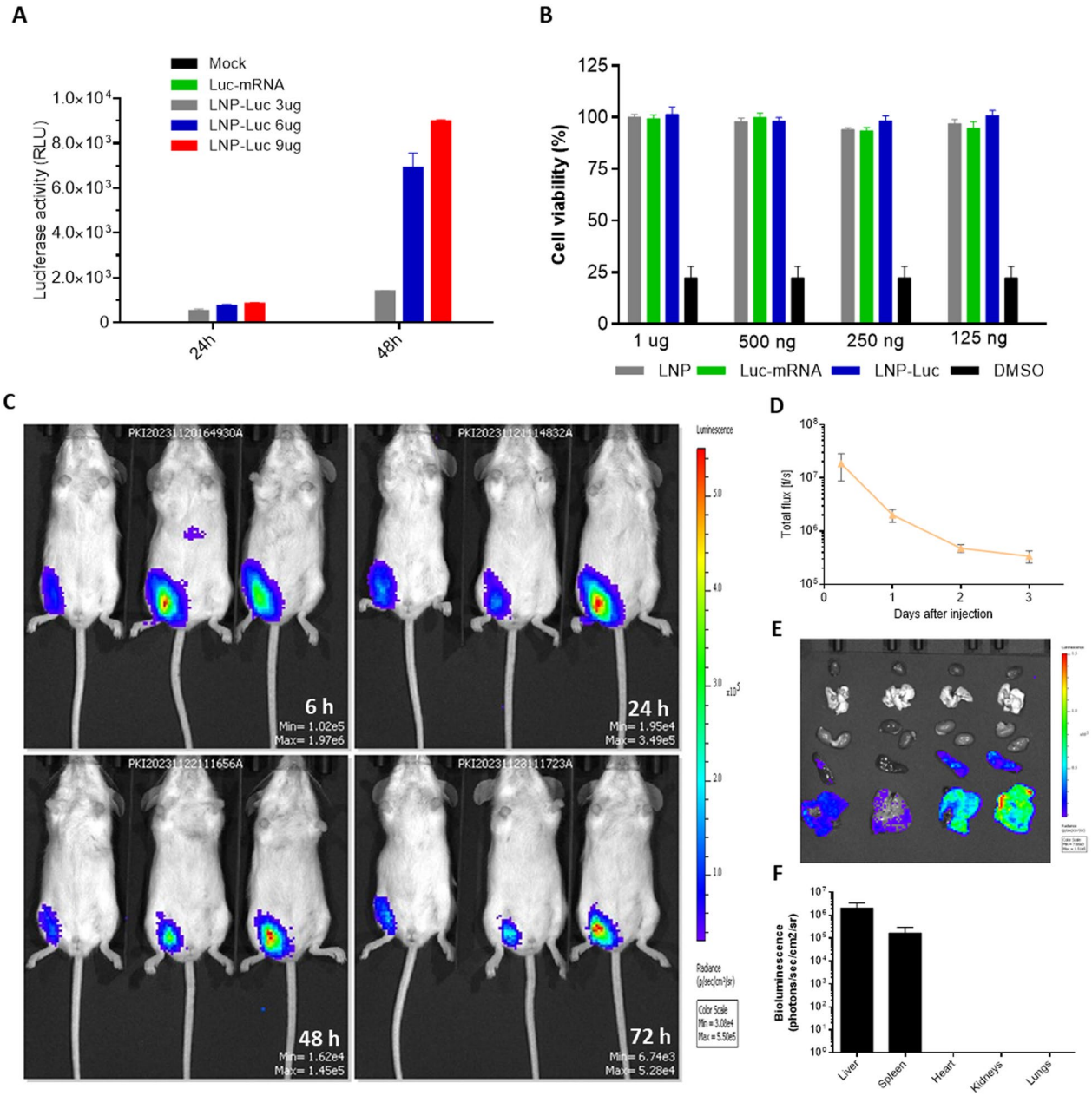

Fig. 2 Delivery of Luc-mRNA in vitro and in vivo. **A** HEK293T cells were transfected with naked Luc-mRNA or 3, 6, or 9 ug with Luc-mRNA encapsulated in LNPs. Twenty-four hours after transfection, cells were collected, and total protein extracts were prepared and used in luciferase assays. **B** Cytotoxicity evaluation of LNP-Luc using sulforhodamine B (SRB) assay. HEK293T cells were treated with different amounts of free or encapsulated mRNA for 24 h. DMSO was used as a positive control for cellular toxicity. **C** In vivo BLI of LNP-Luc in mice. **C** Female BALB/c mice were inoculated with 10 ug of LNP-Luc via IM and subjected to IVIS Spectrum imaging at the indicated times after administration. **D** Tissue distribution of LNP-Luc in mice, and **E** quantification of tissue distribution of LNP-Luc in mice 24 h after administration. **F** Quantification of luminescence expressed in photons per second (p/s) following IM inoculation

Luc-mRNA. As shown in Fig. 2A, low levels of Luc-mRNA expression were detected as early as 24 h only in cells incubated with the RNA formulations. Forty-eight hours post-transfection, a significant increase of luciferase activity was detected in cells transfected with the LNP-mRNA with dose-dependent levels of luciferase activity observed with 3, 6, and 9 μg of LNP-Luc, reaching 9.0×10^4 RLU in cells transfected with 9 μg of encapsulated Luc-RNA. The absence of luciferase activity above background levels in cells incubated with non-encapsulated RNA (naked mRNA) indicated the dependence of the LNP for intracellular delivery of RNA.

To determine the cytotoxicity levels in HEK293T cells, cell viability assays were performed after transfection with different concentrations (125, 250, 500, and 1000 ng) of LNP-Luc and naked mRNA or empty LNP (LNP). The results indicated no toxicity of the LNP formulation with or without encapsulated RNA, as indicated by cell viability that remained at approximately 100% 24 h after transfection (Fig. 2B). Notably, no cellular toxicity was observed even after incubating 4×10^4 cells with 1 ug of LNP-Luc or empty LNP. DMSO was used in the assay as a positive control for cellular toxicity. This result indicates that LNP delivery particle is not only efficient but also safe, as no cell damage was observed.

To visualize the tissue distribution of the LNP-mRNA formulation, LNP-Luc was injected into the muscle thigh of BALB/c mice. Six, 24, 48, and 72 h later, the animals underwent bioluminescence imaging (BLI) analysis. Following IM injection, robust expression of luciferase was mainly concentrated at the site of injection for the course of the experiment (Fig. 2C). Long-term retention of LNP was observed, as the bioluminescence signal was detected for at least up to 3 days after the injection (Fig. 2D). Further ex vivo imaging analysis showed that the liver and spleen present high bioluminescence levels, whereas the heart, kidney, and lungs did not show significant levels of luciferase activity (Fig. 2E, F).

In vivo imaging was also used to examine whether freezing and thawing compromise the Luc mRNA expression. Mice were injected intramuscularly with 10 μg of LNP-Luc seven days after freezing and then underwent IVIS Spectrum imaging 6 h post-injection. No significant changes were observed either in the physicochemical parameters of the formulations or in mRNA integrity (Figures S2D-E), biodistribution pattern, or in vivo bioluminescent signal of the LNPs when compared to freshly prepared ones (Figure S2A-C).

A comparative analysis of LNPs formulated with the two different ionizable lipids, SM-102 or DODMA demonstrated that both formulations exhibit comparable physicochemical parameters based on DLS measurements and %EE analysis (Figure S3). When transfected into HEK293T, in vitro expression analyses of the RNA delivered by the two LNPs indicated that expression levels of the antigen encoded by the RNA are 2 times higher in cells transfected with DODMA-based LNP compared to cells transfected with SM-102-based LNP. When encapsulating Lucifease RNA and inoculated into mice, BLI imaging performed 6 h post-administration, showed similar biodistribution. Taken together, these results further encouraged us to test a DODMA-based LNPs formulation in in vivo studies to determine its potential as a component for novel RNA vaccines (Figure S3).

Evaluation of mice immune response following injection with LNP-mRNA formulations encoding dengue virus and *L. infantum* antigens

To evaluate the immunogenic potential of the LNP-mRNA formulation, we tested two distinct mRNA sequences, one encoding 80% of the E protein (E80) from dengue virus serotype 3 and a second mRNA encoding a *L. infantum* protein known as kinetoplast-associated protein (LinKAP). In the experiments with the dengue virus antigen, plasmid DNA was used as a positive control, as previous data from our group demonstrated that a plasmid DNA vaccine encoding this antigen is highly immunogenic (unpublished). For the Leishmania antigen, prior studies showed that the recombinant protein effectively induces high antibody production (Oliveira et al., submitted). Based on these previous experiments, immunization with the recombinant protein and plasmid DNA were included as positive controls groups for the tests of RNA vaccines for dengue and leishmaniasis. Prior to the LNP preparation, mRNA integrity for both sequences (E80 and LinKAP) was confirmed in denaturing agarose gel electrophoresis, showing an 882 nt band and a 1608 nt band corresponding to the LinKAP and E80 mRNAs, respectively (Fig. 3A). To test in vitro cell delivery and translation efficiency of both LNP formulations, HEK 293 T cells were transfected with the LNP-mRNA, and twenty-four hours later, western blot analyses with transfected cell extracts were performed using anti-dengue antibodies or anti-leishmania LinKAP. As shown in Fig. 3B, transfection with LNP-E80 resulted in the expression of a 47 kDa protein secreted in the culture supernatant, which corresponds to a 429 amino acid protein known to undergo post-translation modifications. Transfection with LNP-LinKAP resulted in the production of a protein with approximately 50 kDa (Fig. 3C). Although the predicted MW of LinKAP protein is 25 kDa, which corresponds to a 235 amino acid protein, anomalous gel mobility in SDS-PAGE, most likely because of the presence of a large repetitive domain, has been previously observed. Taken together, these results

indicate that both LNP-mRNA formulations are highly efficient in delivering functional mRNAs into cells.

To evaluate the immunogenic capacity of the LNP formulations in vivo, we immunized mice with 10 μg of LNP-E80 or LNP-LinKAP. For the LNP-E80, we used a prime-boost protocol, whereas for LNP-LinKAP immunization, we used a prime-boost-boost protocol (Fig. 3D). Twenty days after the first and second immunization with LNP-E80, blood was collected, and total IgG was determined. As shown in Fig. 3E, the immune response induced by E-80 mRNA is comparable with the response induced by plasmid DNA immunization with the corresponding sequence. After prime immunization, mice receiving either LNP-E80 or the pcDNA-E80 produced low levels of total IgG, which showed a significant increase after the second immunization. No significant statistical difference was observed in IgG titers when immunization was compared with pcDNA-E80 or LNP-E80 (Fig. 3E). In contrast, significantly higher levels of IFN-γ produced by mice spleens collected 30 days after the last immunization were detected after immunization with the LNP-E80, compared to mice immunized with pcDNA-E80 plasmid (Fig. 3F).

Regarding immunization with the *Leishmania* antigen, the immune response induced by LinKAP mRNA was compared to that induced by the corresponding recombinant protein: one group of mice was immunized with 10 μg of recombinant LinKAP protein purified from *E. coli,* and one group with the LNP formulation containing 10 μg of LinKAP mRNA. ELISA performed with the recombinant LinKAP protein and sera from immunized animals twenty days after the third immunization showed higher levels of antibodies elicited in mice immunized with LNP-mRNA formulation compared to mice immunized with the recombinant LinKAP protein (Fig. 3G). In contrast, no significant differences in IFN-γ production were observed in mice immunized with the LNP-mRNA or the recombinant protein formulations (Fig. 3H). Taken together, these results showed that, for both dengue virus or a *Leishmania* antigen, immunization protocols with plasmid DNA or a recombinant protein induce similar humoral and cellular immune responses, when compared with immunization with the corresponding LNP-mRNA formulation.

Evaluation of innate immune response

Several studies have shown that lipid nanoparticles are able to enhance the effectiveness of mRNA vaccines by stimulating innate immunity. We evaluated the ability of LNP, with or without mRNA, to stimulate the innate immune response by incubating the nanoparticles with mouse splenocytes and measuring the levels of different cytokines as shown in Fig. 4A. LNPs prepared with the ionizable lipid SM-102, known for its capacity to stimulate innate immunity, were used for comparative analyses [34]. The results demonstrated that both LNPs, prepared with the DODMA or SM-102 lipid, significantly induced TNF production, indicating robust activation of the innate immune response (Fig. 4B). Additionally, we observed significant stimulation in the production of IFN-γ and IL-6 in response to both LNPs. Also, no statistically significant differences between LNP-blank and LNP-mRNA were observed. In contrast, naked mRNA did not induce the production of any of the evaluated cytokines, highlighting the role of lipids as an essential component of mRNA vaccines for effective innate immune activation. The absence of IL-10 production, an anti-inflammatory cytokine, is an interesting outcome as it suggests that LNP do not trigger an anti-inflammatory response that could attenuate the desired immunological efficacy. Furthermore, IL-2, IL-4, and IL-17 were not detected in any of the conditions tested (data not shown). These findings suggest that the new LNP formulation used in our studies is effective in inducing initial inflammatory responses characterized by the production of proinflammatory cytokines such as TNF, IFN-γ, and IL-6, which is important to the adjuvant activity of the delivery system and the efficacy of mRNA vaccines [24].

Discussion

The indisputable success of the COVID-19 vaccines and the urgent need to develop other vaccines for infectious diseases, particularly those affecting the population in less developed countries, have prompted many groups

(See figure on next page.)

Fig. 3 In vitro expression of LNP mRNAs and in vivo immunogenicity **A** mRNA from two different antigens (E80 dengue virus serotype 3 and LinKAP from *Leishmania*) were in vitro synthesized and HEK293T cells were transfected with both LNP-mRNAs respectively. Forty-eight hours after transfection, cells were collected, and a Western blot was performed with **B** culture supernatant from cells transfected with E80 or **C** total protein extract from cells transfected with LinKAP. **D** Female C57BL/6 mice were immunized IM with 10 μg of LNP-E80 or LNP-LinKAP, naked mRNA or empty-LNP, with a prime-boost or prime-boost-boost regimen at a 3-week interval. Serum was collected on days 20, 41 and 62 to analyze specific total IgG. **E** Total IgG titers after mice immunization with LNP-E80 after the boost ($p < 0.0001$). Thirty days after the last immunization, mice spleens were collected and used in splenocyte cultures with the appropriate stimuli. **F** IFN-γ production in mice immunized with LNP-E80 (****$p < 0.0001$, ***$p < 0.001$). **G** Total IgG titers after mice immunization with LNP-LinKAP ($p < 0.0001$). **H** IFN-γ production in mice immunized with LNP-LinKAP (**$p = 0.0001$, *$p = 0.0001$). Statistical analysis was performed with 2-way ANOVA with Turkey's multiple comparisons test

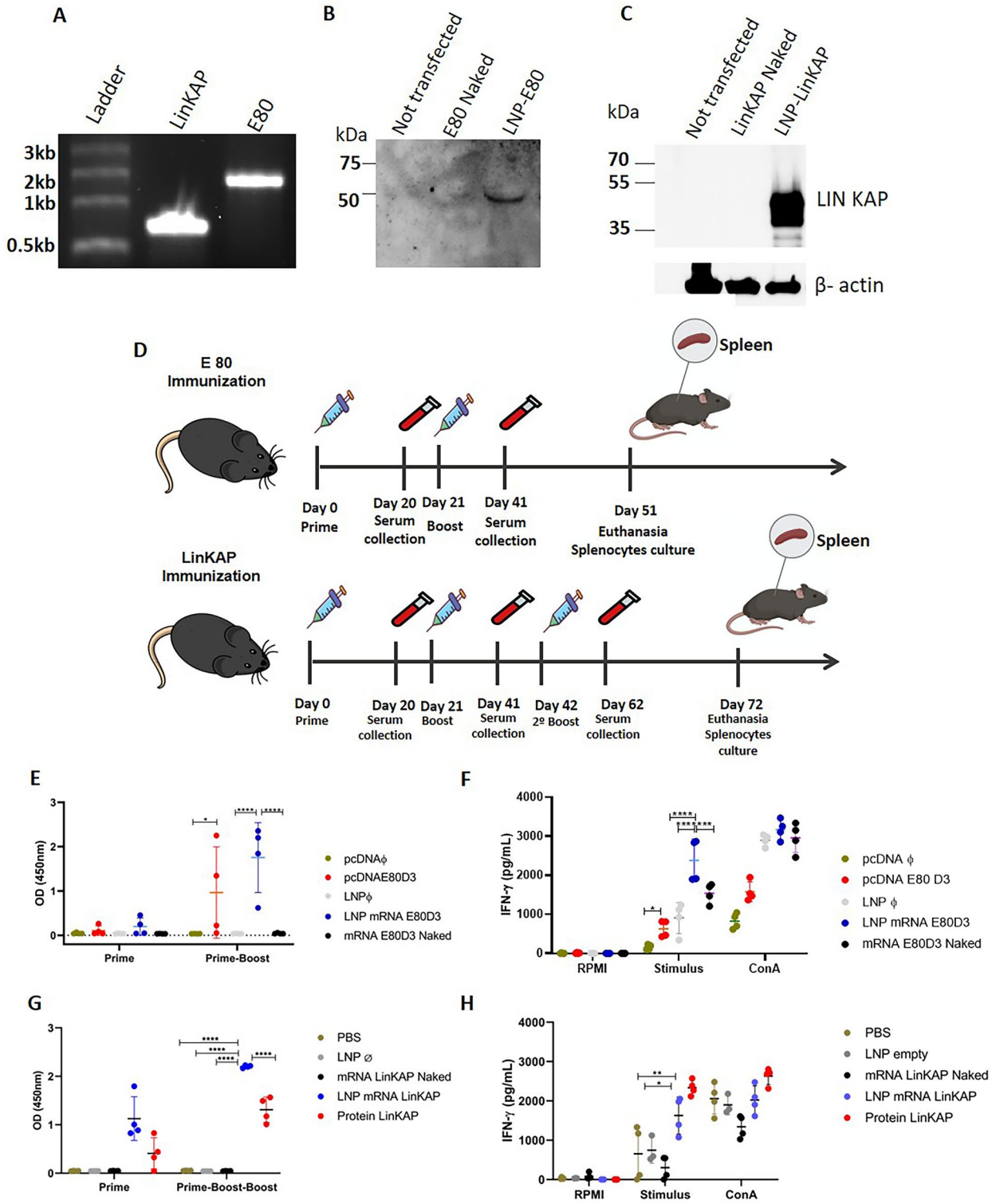

Fig. 3 (See legend on previous page.)

to invest in nucleic acid-based vaccines, notably mRNA vaccines. In this work, we successfully designed and generated a novel LNP formulation capable of encapsulating mRNAs encoding two distinct antigens. For both antigens tested, the dengue virus envelope protein and an immunogenic protein present in different *Leishmania*

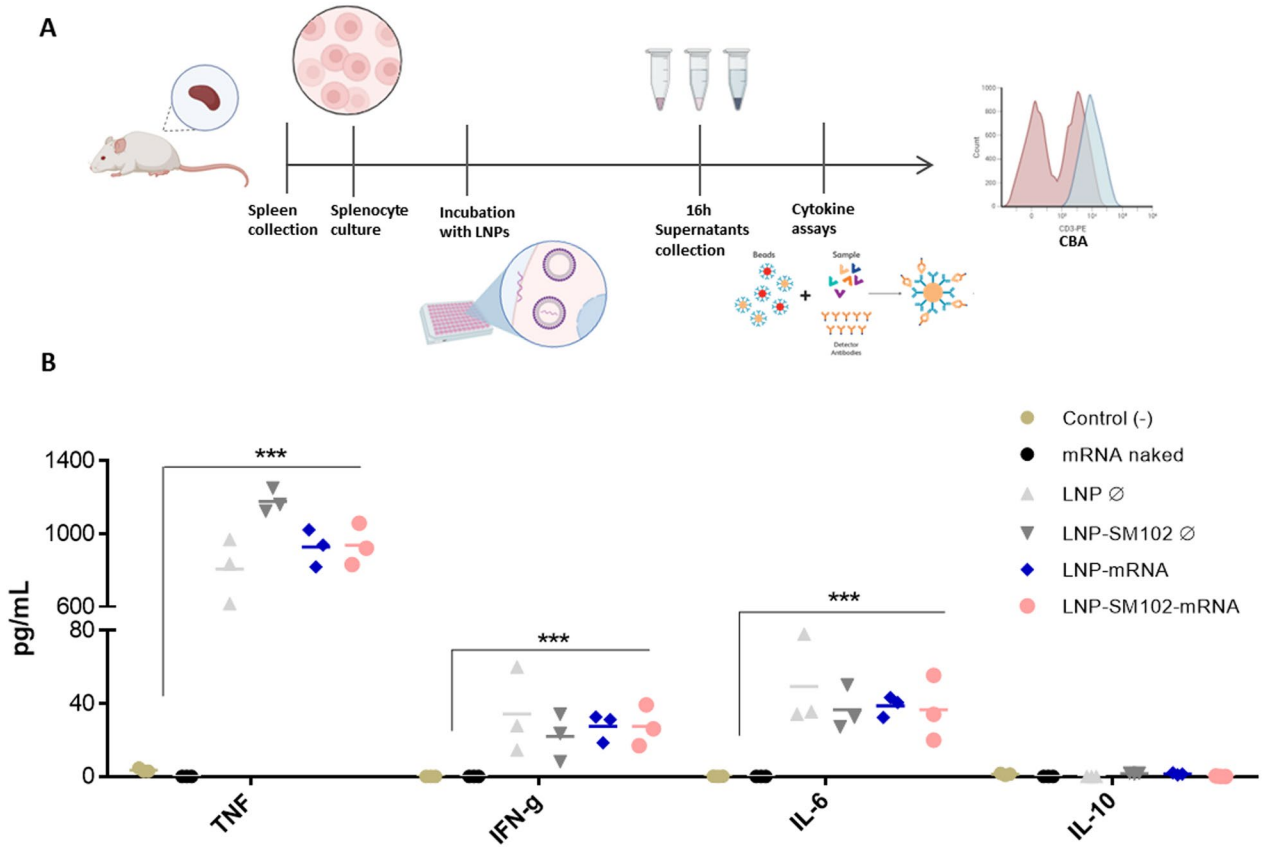

Fig. 4 Evaluation of innate immune response. **a** Splenocytes were isolated from Balb/c naïve mice and stimulated with either empty or mRNA-loaded, or naked mRNA. Sixteen hours post-incubation, cytokine levels were measured using the CBA Mouse Th1/Th2/Th17 kit. **b** Cytokine production in response to LNP with or without mRNA and SM-102. Mouse splenocyte cultures were stimulated with LNP, and cytokine levels were measured 16 h after incubation for TNF, IFN-γ, IL-6, IL-10, IL-2, IL-4, and IL-17

species, we showed that the novel LNP-mRNA formulations are safe and highly immunogenic.

One of the main challenges for developing mRNA vaccines is the production of LNP that can efficiently deliver the mRNA into APC. When defining the components of an LNP, the choice of the ionizable lipid is crucial since a variety of ionizable lipid formulations with high encapsulation efficiency have been tested during the development of many different mRNA vaccines. While DODMA is not a novel lipid and has been reported in previous research, its application in LNP for mRNA-based vaccines represents an unexplored area of significant potential. Besides, the current ionizable lipids used in the commercially available vaccines are under patent protection. In our studies, DODMA was chosen as an ideal ionizable lipid due to its advantageous attributes, including its chemical structure and a pKa value of 6.59 (determined via TNS binding assay), which facilitate efficient LNP formation, membrane fusion, and endosomal escape [35, 36]. Furthermore, it is commercially available, simplifying the production process, and, in the context of ongoing vaccine development, it can be subjected to intellectual property protection. To our knowledge, it is the first time that DODMA is employed as an ionizable lipid for mRNA delivery in mRNA-based vaccines.

Evaluation of the physical properties of the delivery system showed an average particle size of about 100 nm, $D90 \leq 200$ nm, regardless of the encapsulated mRNA. For LNP uptake by dendritic cells, ideal particle sizes are 20–200 nm, whereas particle sizes between 500 and 5000 nm are preferentially taken up by macrophages [26].

The zeta potential was close to neutrality, slightly negative, as expected, due to the presence of the PEG layer, DPSC, and cholesterol. At physiological pH, the excess ionizable lipid is no longer protonated, thereby not providing a positive charge to the system. LNPs with a negative zeta potential are less toxic and immunostimulatory than those with a cationic zeta potential. Positively charged LNP can trigger an immune response, leading to inflammation and potential tissue damage [17]. In a previous study, the apparent pKa of LNP composed of DODMA:cholesterol:DSPC:DMG-PEG in a ratio of

50:38.5:10:1.5 was determined to be approximately 6.41 using the TNS binding assay [36]. This finding indicates that the addition of lipids in the formulation has a minimal effect on the overall pKa value. Importantly, this pKa value significantly facilitates mRNA delivery in vivo, as it influences membrane fusion and endosomal escape.

Cryo-TEM images showed homogeneous circular structures with a semi-structured lipid bilayer and an electron-dense nucleus. Currently, it is believed that LNP-mRNAs are consistent with the core–shell model, characterized by a surface layer and an amorphous, isotropic core. Studies indicate two possible core types: an amorphous core containing water pores surrounded by inverted cationic lipids or homogeneously dispersed lipids with small water pockets [13, 37]. The mRNA is housed within bleb compartments, distinguished by their characteristic mottled mass density [38]. The CryoTEM analyses shown here are consistent with the results with dioleic LNPs, where each lipid tail contains only one double bond (C18-1 double bond) (DODMA, DODAP), which revealed LNP populations with a high frequency of small liposomal structures [17].

The efficacy of mRNA vaccine depends on protein antigen expression followed by an antigen-specific immune response [10, 12]. Delivery of large mRNA transcripts remains an important consideration for the development of vaccines. We showed that all three LNP-mRNA formulations can efficiently deliver mRNAs into cells, yielding detectable protein expression levels as early as 24 h post-transfection of cell cultures. In contrast to naked mRNA, which is barely transfected into immortalized cell lines unless complexed with cationic polymer or lipid-based reagents, such as TransIT or Lipofectin [12], the LNP itself functions as a transfection reagent, aiding in the seamless entry of mRNA into the cellular cytoplasm through endocytic pathways. For effective transfection, mRNA must escape the endosomes before they fuse with lysosomes, and the mRNA is degraded [39]. In contrast to a few studies indicating that LNP-mRNA may cause cytotoxicity, including oxidative stress and apoptosis [40], we showed that, besides efficient transfection, the LNP-Luc formulation has no toxicity for the transfected cell.

Besides high protein expression levels after in vitro transfection, mice injection with LNP-Luc also demonstrated that this formulation results in adequate biodistribution and highly efficient kinetics. Similar to the results obtained with other LNP formulations [12, 41–43], upon IM injection, robust protein expression was readily detected in the muscle tissue at the injection site and the two most predominant expression sites, the liver, and spleen (Fig. 2C–F). It has been demonstrated that once injected intramuscularly, APC, including neutrophils, monocytes, macrophages, and dendritic cells, efficiently internalize LNPs at both the injection site and the adjacent draining lymph nodes [26]. Uptake by the liver and spleen was expected since most nanoparticles are cleared from blood vessels and trapped off-target in the mononuclear phagocyte system after administration [44]. It is important to note that the LNP-Luc formulation was found to be stable at 4°C and after at least seven days post-freezing. When stored in a cryoprotective buffer containing tris-sucrose 12%, LNP-Luc was shown to maintain not only all physical properties but also the capacity to deliver the mRNA with similar efficiency compared to the freshly prepared formulation. The advantage of having a stable mRNA vaccine formulation at 4 °C is worth noting, particularly if we consider the development of vaccines to be delivered in areas where cold-chain control is harder to achieve.

LNPs act as adjuvant by activating innate immune cells such as APCs, regardless of the presence of encapsulated mRNA. Alameh et al. (2021) found that LNPs, regardless of the encapsulated mRNA, induce follicular helper T cell (Tfh cell), B cell, and humoral responses in mice. IL-6 induction and the ionizable lipid component are key for this adjuvant activity, eliminating the need for additional adjuvants in mRNA vaccines [24, 27–32]. Evidence of activation of innate immune cells, the LNP formulation stimulated naïve splenocytes to produce proinflammatory cytokines such as TNF, IFN-γ and IL-6 in vitro, even in the absence of encapsulated mRNA. In contrast, the production of anti-inflammatory cytokines such as IL-10 was not detected. This cytokine profile was similar to that induced by LNPs containing a lipid composition used in commercially available mRNA vaccines.

Finally, we tested antigens from dengue virus and *Leishmania* parasites. These two pathogens were chosen based on previous studies indicating that protection is mediated by antibodies and T cells, respectively. After encapsulation into LNPs, mRNAs encoding either the E80 protein from dengue or the LinKAP from *L. infantum* were able to induce strong humoral and T cell responses, as shown by the high titers of circulating antibodies and IFN-γ produced by T lymphocytes. In contrast to COVID-19 and malaria, only limited studies describing mRNA vaccines for leishmaniasis and dengue infection have been published [45, 46]. This contrasts with a long list of studies using recombinant protein and plasmid DNA as a vaccine platform for protection against dengue virus and various *Leishmania* species [47–52]. Of note, immunization of LNP-LinKAP induced higher titers of antibodies and similar levels of *ex-vivo* IFN-γ compared to immunization with the corresponding adjuvanted recombinant protein. Likewise, IgG titers and IFNγ levels were similar when comparing mice immunized with either LNP-mRNA or plasmid DNA in the case of the dengue virus

antigen. Since IgG levels and IFN-γ production correlate with protection against multiple infectious agents, these novel LNP-mRNA formulations are likely to be protective against a wide variety of pathogens.

The selection of two distinct antigens—one viral and one protozoan—highlights the versatility of the formulation and paves the way for the development of an mRNA-based vaccine platform using nanoparticles containing DODMA. This innovative formulation, capable of efficiently encapsulating new antigens and eliciting robust immune responses, marks a significant step forward in advancing the creation of novel mRNA-based vaccines, particularly for neglected diseases.

Conclusion

Here, we developed and characterized LNP loaded with luciferase mRNA and mRNAs encoding two different antigens. This novel nano platform effectively delivered the mRNA to cells and was detected in vivo for at least 3 days following a single injection. Immunogenicity studies showed the efficient induction of specific antibody responses and cellular immunity for both evaluated antigens. Although further preclinical studies are required, the data obtained thus far indicate that this LNP composition may be a promising platform for developing mRNA-based vaccines against various diseases.

Abbreviations

LNP	Lipid nanoparticles
mRNA	Messenger RNA
APC	Antigen-presenting cells
PEG	Polyethylene glycol
IL	Interleukin
LinKAP	Leishmania infantum Kinetoplast Associated Protein
E80	80% Of the dengue serotype 3 E protein
DODMA	1,2-Dioleyloxy-3-dimethylaminopropane
DSPC	1,2–Distearoyl-sn-glycero-3-phosphocholine
DMG-PEG-2000	1,2-Dimyristoyl-rac-glycero-3-methoxypolyethylene glycol-2000
Luc	Luciferase
PDI	Polydispersity index
DLS	Dynamic light scattering
NTA	Nanoparticle tracking analysis
SRB	Sulforhodamine B
DMSO	Dimethylsulfoxide
IM	Intramuscular
TMB	3.3′5.5.5-Tetramethylbenzidine
Cryo-TEM	Cryogenic transmission electron microscopy
%EE	Encapsulation efficiency
RLU	Relative light unit
TNF	Tumor necrosis factor
IFN-γ	Interferon-gamma

Supplementary Information

The online version contains supplementary material available at https://doi.org/10.1186/s12951-025-03201-8.

Supplementary file 1: Figure S1. Sequences of viral and parasite antigens. DNA coding region from E80 was used to transcribe E80 mRNA with signal peptide from *Homo sapiens* plasminogen activator (nucleotides 1 to 105), and the partial sequence of *Leishmania* antigen LIN-KAP was used in the experiments. Figure S2. Freeze-Thaw Stability of LNP-Luc. Female BALB/c mice were inoculated with 10 µg of LNP-Luc via IM and subjected to IVIS Spectrum imaging 6 hours after administration of (a) freshly prepared LNP-Luc in PBS and (b) seven days post-freezing LNP-Luc in tris-sucrose 12%. (c) Quantification of luminescence expressed in photons per second (p/s) following IM inoculation. (d) Analysis of Luc mRNA in agarose gel in denaturing conditions: 1- mRNA-Luc extracted from freshly prepared LNP-Luc and 2- mRNA-Luc extracted from seven days post-freezing LNP-Luc. (e) Mean diameter, polydispersity index (PDI), zeta potential, encapsulation efficiency (%EE) for both administered LNP-Luc. Figure S3. Comparative physicochemical characterization and biodistribution of LNPs containing DODMA and SM-102. (A) Mean diameter, polydispersity index (PDI), zeta potential, and encapsulation efficiency (%EE) of LNP-DODMA and LNP-SM102 encapsulating luciferase mRNA. (B) HEK 293T cells were transfected with LNP-LinKAP formulated with either DODMA or SM-102. Forty-eight hours post-transfection, the cells were harvested, and total protein extracts were prepared for Western blot analysis. The lanes were loaded as follows: 1 – negative control (non-transfected cells), 2 – naked mRNA, 3 – LNP-LinKAP (DODMA), 4 – LNP-LinKAP (SM-102). (C) *In vivo* BLI of LNP-Luc in mice. Female BALB/c mice were inoculated with 10 µg of LNP-Luc via IM and subjected to IVIS Spectrum imaging 6 hours after administration of LNP-Luc (DODMA) and LNP-Luc (SM-102).

Acknowledgements

The authors wish to thank the staff from the Microscopy and Image Microanalysis Platform from Rene Rachou Institute/Fiocuz for their technical support with the bioluminescent analyses. We also thank the staff of the LNNano/CNPEM for the access to the electron microscopy facility and technical support in the execution of the analyses. We thank Prof. Norbert Pardi from University of Pennsylvania for providing us with plasmid pUC-TEV-luc2deltaE-arl used as a template to produce luciferase mRNA and professor Luís Carlos Ferreira from USP for the technical support in experiments involving luciferase mRNA. This work received funds from the Conselho Nacional de Desenvolvimento Científico e Tecnológico (CNPq, 407958/2022-3), Coordenação de Aperfeiçoamento de Pessoal de Nível Superior (CAPES), Fundação de Amparo à Pesquisa de Minas Gerais (FAPEMIG) and The Instituto Nacional de Ciência e Tecnologia de Vacinas (INCTV).

Author contributions

RSF and GBC: Conceptualization, Methodology, Validation, Formal analyses, Investigation, Data Curation, Prepared Figures, Wrote Original Draft, Reviewed & Edited. SSR: Methodology, Formal analyses, Investigation, Data Curation. AFB: Methodology, Formal analyses, Investigation, Data Curation. NPSL: Methodology, Formal analyses. MP: Methodology, Investigation. Formal analyses, Reviewed & Edited. JOS: Methodology, Investigation, Data Curation. NSHS: Methodology, Investigation, Data Curation. IVC: Methodology, Investigation, Data Curation. BO: Methodology, Investigation, Data Curation. APF: Conceptualization, Formal analyses, Resources, Funding acquisition. FGF: Conceptualization, Formal analyses, Resources. RTG: Conceptualization, Formal analyses, Resources, Funding acquisition. DSF: Conceptualization, Formal analyses, Wrote Original Draft, Reviewed & Edited, Supervision. SMR: Conceptualization, Resources, Formal analyses, Wrote Original Draft, Reviewed & Edited the manuscript, Prepared Figures, Supervision, Project administration, Funding acquisition. All authors reviewed the manuscript.

Data availability

No datasets were generated or analysed during the current study.

Declarations

Competing interests

The authors declare no competing interests.

Author details

[1]Centro de Tecnologia de Vacinas da, Universidade Federal de Minas Gerais, Belo Horizonte, Belo Horizonte, MG 31310-260, Brazil. [2]Department of Pharmaceuticals, School of Pharmacy, Universidade Federal de Minas Gerais, Belo

Horizonte, MG 31270-901, Brazil. [3]Instituto René Rachou, Fundação Oswaldo Cruz-Minas, Belo Horizonte, MG 30190-002, Brazil. [4]Department of Microbiology, Institute of Biological Sciences, Universidade Federal de Minas Gerais, Belo Horizonte, MG 31270-901, Brazil. [5]Department of Biochemistry & Immunology, Institute of Biological Sciences, Universidade Federal de Minas Gerais, Belo Horizonte, MG 31270-901, Brazil. [6]Department of Clinical & Toxicological Analysis, School of Pharmacy, Universidade Federal de Minas Gerais, Belo Horizonte, MG 31270-901, Brazil.

Received: 17 August 2024 Accepted: 4 February 2025
Published online: 18 March 2025

References

1. Fire A, Xu S, Montgomery MK, Kostas SA, Driver SE, Mello CC. Potent and specific genetic interference by double-stranded RNA in Caenorhabditis elegans. Nature. 1998;391(6669):806–11.
2. Kon E, Elia U, Peer D. Principles for designing an optimal mRNA lipid nanoparticle vaccine. Curr Opin Biotechnol. 2022;73:329–36.
3. Hassett KJ, Benenato KE, Jacquinet E, Lee A, Woods A, Yuzhakov O, Himansu S, DeterLing J, Geilich BM, Ketova T, Mihai C, Lynn A, McFadyen I, Moore MJ, Senn JJ, Stanton MG, Almarsson O, Ciaramella G, Brito LA. Optimization of lipid nanoparticles for intramuscular administration of mrna vaccines. Mol Ther Nucleic Acids. 2019;15:1–11.
4. Jackson NAC, Kester KE, Casimiro D, Gurunathan S, DeRosa F. The promise of mRNA vaccines: a biotech and industrial perspective. NPJ Vaccines. 2020;5:11.
5. Pilkington EH, Suys EJA, Trevaskis NL, Wheatley AK, Zukancic D, Algarni A, Al-Wassiti H, Davis TP, Pouton CW, Kent SJ, Truong NP. From influenza to COVID-19: lipid nanoparticle mRNA vaccines at the frontiers of infectious diseases. Acta Biomater. 2021;131:16–40.
6. Rzymski P, Szuster-Ciesielska A, Dzieciatkowski T, Gwenzi W, Fal A. mRNA vaccines: the future of prevention of viral infections? J Med Virol. 2023;95(2): e28572.
7. Kariko K, Buckstein M, Ni H, Weissman D. Suppression of RNA recognition by toll-like receptors: the impact of nucleoside modification and the evolutionary origin of RNA. Immunity. 2005;23(2):165–75.
8. Karam M, Daoud G. mRNA vaccines: past, present, future. Asian J Pharm Sci. 2022;17(4):491–522.
9. Kim SC, Sekhon SS, Shin WR, Ahn G, Cho BK, Ahn JY, Kim YH. Modifications of mRNA vaccine structural elements for improving mRNA stability and translation efficiency. Mol Cell Toxicol. 2022;18:1–8.
10. Pardi N, Hogan MJ, Porter FW, Weissman D. mRNA vaccines. a new era in vaccinology. Nat Rev Drug Discov. 2018;17(4):261–79.
11. Hou X, Zaks T, Langer R, Dong Y. Lipid nanoparticles for mRNA delivery. Nat Rev Mater. 2021;6(12):1078–94.
12. Pardi N, Tuyishime S, Muramatsu H, Kariko K, Mui BL, Tam YK, Madden TD, Hope MJ, Weissman D. Expression kinetics of nucleoside-modified mRNA delivered in lipid nanoparticles to mice by various routes. J Control Release. 2015;217:345–51.
13. Schoenmaker L, Witzigmann D, Kulkarni JA, Verbeke R, Kersten G, Jiskoot W, Crommelin DJA. mRNA-lipid nanoparticle COVID-19 vaccines: structure and stability. Int J Pharm. 2021;601: 120586.
14. Liang F, Lindgren G, Lin A, Thompson EA, Ols S, Rohss J, John S, Hassett K, Yuzhakov O, Bahl K, Brito LA, Salter H, Ciaramella G, Lore K. Efficient targeting and activation of antigen-presenting cells In Vivo after modified mRNA vaccine administration in rhesus macaques. Mol Ther. 2017;25(12):2635–47.
15. Lindsay KE, Bhosle SM, Zurla C, Beyersdorf J, Rogers KA, Vanover D, Xiao P, Arainga M, Shirreff LM, Pitard B, Baumhof P, VilLinger F, Santangelo PJ. Visualization of early events in mRNA vaccine delivery in non-human primates via PET-CT and near-infrared imaging. Nat Biomed Eng. 2019;3(5):371–80.
16. Gote V, Bolla PK, Kommineni N, Butreddy A, Nukala PK, Palakurthi SS, Khan W. A comprehensive review of mRNA vaccines. Int J Mol Sci. 2023;24(3):2700.
17. Cheng X, Lee RJ. The role of helper lipids in lipid nanoparticles (LNPs) designed for oligonucleotide delivery. Adv Drug Deliv Rev. 2016;99(Pt A):129–37.
18. Han X, Zhang H, Butowska K, Swingle KL, Alameh MG, Weissman D, Mitchell MJ. An ionizable lipid toolbox for RNA delivery. Nat Commun. 2021;12(1):7233.
19. Eygeris Y, Gupta M, Kim J, Sahay G. Chemistry of lipid nanoparticles for RNA delivery. Acc Chem Res. 2022;55(1):2–12.
20. Albertsen CH, Kulkarni JA, Witzigmann D, Lind M, Petersson K, Simonsen JB. The role of lipid components in lipid nanoparticles for vaccines and gene therapy. Adv Drug Deliv Rev. 2022;188:114416.
21. Maeki M, Fujishima Y, Sato Y, Yasui T, Kaji N, Ishida A, Tani H, Baba Y, Harashima H, Tokeshi M. Understanding the formation mechanism of lipid nanoparticles in microfluidic devices with chaotic micromixers. PLoS ONE. 2017;12(11): e0187962.
22. Maeki M, Uno S, Niwa A, Okada Y, Tokeshi M. Microfluidic technologies and devices for lipid nanoparticle-based RNA delivery. J Control Release. 2022;344:80–96.
23. Evers MJW, Kulkarni JA, van der Meel R, Cullis PR, Vader P, Schiffelers RM. State-of-the-art design and rapid-mixing production techniques of lipid nanoparticles for nucleic acid delivery. Small Methods. 2018;2:1700375.
24. Verbeke R, Hogan MJ, Lore K, Pardi N. Innate immune mechanisms of mRNA vaccines. Immunity. 2022;55(11):1993–2005.
25. Reichmuth AM, Oberli MA, Jaklenec A, Langer R, Blankschtein D. mRNA vaccine delivery using lipid nanoparticles. Ther Deliv. 2016;7(5):319–34.
26. Hassett KJ, Higgins J, Woods A, Levy B, Xia Y, Hsiao CJ, Acosta E, Almarsson O, Moore MJ, Brito LA. Impact of lipid nanoparticle size on mRNA vaccine immunogenicity. J Control Release. 2021;335:237–46.
27. Chatzikleanthous D, O'Hagan DT, Adamo R. Lipid-based nanoparticles for delivery of vaccine adjuvants and antigens: toward multicomponent vaccines. Mol Pharm. 2021;18(8):2867–88.
28. Awasthi S, Hook LM, Pardi N, Wang F, Myles A, Cancro MP, Cohen GH, Weissman D, Friedman HM. Nucleoside-modified mRNA encoding HSV-2 glycoproteins C, D, and E prevents cLinical and subcLinical genital herpes. Sci Immunol. 2019;4(39):eaaw7083.
29. Shirai S, Kawai A, Shibuya M, Munakata L, Omata D, Suzuki R, Yoshioka Y. Lipid nanoparticle acts as a potential adjuvant for influenza split vaccine without inducing inflammatory responses. Vaccines. 2020;8(3):433.
30. Tahtinen S, Tong AJ, Himmels P, Oh J, Paler-Martinez A, Kim L, Wichner S, Oei Y, McCarron MJ, Freund EC, Amir ZA, de la Cruz CC, Haley B, Blanchette C, Schartner JM, Ye W, Yadav M, Sahin U, Delamarre L, Mellman I. IL-1 and IL-1ra are key regulators of the inflammatory response to RNA vaccines. Nat Immunol. 2020;4:532–42.
31. Ndeupen S, Qin Z, Jacobsen S, Bouteau A, Estanbouli H, Igyártó BZ. The mRNA-LNP platform's lipid nanoparticle component used in precLinical vaccine studies is highly inflammatory. IScience. 2021;24(12): 103479.
32. Alameh MG, Tombacz I, Bettini E, Lederer K, Sittplangkoon C, Wilmore JR, Gaudette BT, Soliman OY, Pine M, Hicks P, Manzoni TB, Knox JJ, Johnson JL, Laczko D, Muramatsu H, Davis B, Meng W, Rosenfeld AM, Strohmeier S, Lin PJC, Mui BL, Tam YK, Kariko K, Jacquet A, Krammer F, Bates P, Cancro MP, Weissman D, Luning Prak ET, Allman D, Locci M, Pardi N. Lipid nanoparticles enhance the efficacy of mRNA and protein subunit vaccines by inducing robust T follicular helper cell and humoral responses. Immunity. 2021;54(12):2877–28922877.
33. Al Fayez N, Nassar MS, Alshehri AA, Alnefaie MK, Almughem FA, Alshehri BY, Alawad AO, Tawfik EA. Recent advancement in mRNA vaccine development and applications. Pharmaceutics. 2023;15(7):1972.
34. Zhang L, More KR, Ojha A, Jackson CB, Quinlan BD, Li H, He W, Farzan M, Pardi N, Choe H. Effect of mRNA-LNP components of two globally-marketed COVID-19 vaccines on efficacy and stability. NPJ Vaccines. 2023;8:156.
35. Sun D, Lu ZR. Structure and function of cationic and ionizable lipids for nucleic acid delivery. Pharm Res. 2023;40(1):27–46.
36. Carrasco MJ, Alishetty S, Alameh MG, Said H, Wright L, Paige M, Soliman O, Weissman D, Cleveland TE 4th, Grishaev A, Buschmann MD. Ionization and structural properties of mRNA lipid nanoparticles influence expression in intramuscular and intravascular administration. Commun Biol. 2021;4(1):956.
37. Viger-Gravel J, Schantz A, Pinon AC, Rossini AJ, Schantz S, Emsley L. Structure of lipid nanoparticles containing siRNA or mRNA by dynamic nuclear polarization-enhanced NMR spectroscopy. J Phys Chem B. 2018;122(7):2073–81.

38. Brader ML, Williams SJ, Banks JM, Hui WH, Zhou ZH, Jin L. Encapsulation state of messenger RNA inside lipid nanoparticles. Biophys J. 2021;120(14):2766–70.
39. Alvarez-Benedicto E, Farbiak L, Marquez Ramirez M, Wang X, Johnson LT, Mian O, Guerrero ED, Siegwart DJ. Optimization of phospholipid chemistry for improved lipid nanoparticle (LNP) delivery of messenger RNA (mRNA). Biomater Sci. 2022;10(2):549–59.
40. Paramasivam P, Franke C, Stoter M, Hoijer A, Bartesaghi S, Sabirsh A, Lindfors L, Arteta MY, Dahlen A, Bak A, Andersson S, Kalaidzidis Y, Bickle M, Zerial M. Endosomal escape of delivered mRNA from endosomal recycling tubules visualized at the nanoscale. J Cell Biol. 2022. https://doi.org/10.1083/jcb.202110137.
41. Bahl K, Senn JJ, Yuzhakov O, Bulychev A, Brito LA, Hassett KJ, Laska ME, Smith M, Almarsson O, Thompson J, Ribeiro AM, Watson M, Zaks T, Ciaramella G. Preclinical and clinical demonstration of immunogenicity by mRNA vaccines against H10N8 and H7N9 influenza viruses. Mol Ther. 2017;25(6):1316–27.
42. Zhang NN, Li XF, Deng YQ, Zhao H, Huang YJ, Yang G, Huang WJ, Gao P, Zhou C, Zhang RR, Guo Y, Sun SH, Fan H, Zu SL, Chen Q, He Q, Cao TS, et al. A Thermostable mRNA Vaccine against COVID-19. Cell. 2020;182(5):1271-1283 e1216.
43. Elia U, Ramishetti S, Rosenfeld R, Dammes N, Bar-Haim E, Naidu GE, Makdasi E, Yahalom-Ronen Y, Tamir H, Paran N, Cohen O, Peer D. Design of SARS-CoV-2 hFc-conjugated receptor-binding domain mRNA vaccine delivered via lipid nanoparticles. ACS Nano. 2021;15(6):9627–37.
44. Ngo W, Ahmed S, Blackadar C, Bussin B, Ji Q, Mladjenovic SM, Sepahi Z, Chan WCW. Why nanoparticles prefer liver macrophage cell uptake in vivo. Adv Drug Deliv Rev. 2022;185: 114238.
45. Wollner CJ, Richner M, Hassert MA, Pinto AK, Brien JD, Richner JM. A dengue virus serotype 1 mRNA-LNP vaccine elicits protective immune responses. J Virol. 2021;95(12):e02482-e2520.
46. Duthie MS, Machado BAS, Badaró R, Kaye PM, Reed SG. Leishmaniasis vaccines: applications of RNA technology and targeted clinical trial designs. Pathogens. 2022;11(11):1259.
47. Gomes DCO, Souza BLSC, Schwedersky RP, Covre LP, Guedes HLM, Lopes UG, Ré MI, Rossi-Bergmann B. Intranasal immunization with chitosan microparticles enhances LACK-DNA vaccine protection and induces specific long-lasting immunity against visceral leishmaniasis. Microbes Infect. 2022;24(2): 104884.
48. He J, Huang F, Zhang J, Chen H, Chen Q, Zhang J, Li J, Zheng Z, Chen D, Chen J. DNA prime-protein boost vaccine encoding HLA-A2, HLA-A24 and HLA-DR1 restricted epitopes of CaNA2 against visceral leishmaniasis. Immunology. 2019;156(1):94–108.
49. Emerick SO, de Carvalho TV, Miranda BM, da Silva AC, Martins TVF, de Oliveira LL, Marques-da-Silva EA. Lipophosphoglycan-3 protein from Leishmania infantum chagasi plus saponin adjuvant: a new promising vaccine against visceral leishmaniasis. Vaccine. 2021;39(2):282–91.
50. Imagawa T, Ito M, Matsuda M, Nakashima K, Tokunaga Y, Ohta Y, Li TC, Suzuki R, Suzuki T. Virus-like particles with FLAG-tagged envelope protein as a tetravalent dengue vaccine candidate. Sci Rep. 2021;11(1):17542.
51. Dixit NK. Design of monovalent and chimeric tetravalent dengue vaccine using an immunoinformatics approach. Int J Pept Res Ther. 2021;27(4):2607–24.
52. Torres-Flores JM, Reyes-Sandoval A, Salazar MI. Dengue vaccines: an update. BioDrugs. 2022;36(3):325–36.

Publisher's Note